Liquid-Crystalline Supramolecular Polymers Formed through Complementary Nucleobase-Pair Interactions

Sona Sivakova,[a] Jian Wu,[b] Cheryl J. Campo,[a] Patrick T. Mather,[a] and Stuart J. Rowan*[a]

Abstract: We report how the placement of nucleobase units, thymine, or N^6-(4-methoxybenzoyl)adenine, onto the ends of a mesogenic core, bis-4-alkoxy-substituted bis(phenylethynyl)-benzene, affects the properties of these materials. We show that addition of these bulky polar groups significantly reduces the range of liquid-crystalline behavior of these compounds. However, mixing two complementary nucleobase-containing AA- and BB-type monomer units together does result in

Keywords: hydrogen bonds · liquid crystals · nucleobases · polymers · supramolecular chemistry

the formation of stable, thermotropic liquid-crystalline (LC) phases. Hydrogen bonding is shown to play an important role in the formation of these LC phases, consistent with the formation of oligomeric or polymeric hydrogen-bonded aggregates. X-ray analyses of these mixed materials are consistent with the formation of smectic C phases.

Introduction

Over the last decade, supramolecular polymerization, that is, the self-assembly of small monomeric units into polymer-like materials through the use of noncovalent interactions, has received growing attention.[1] Conceptually, a simple way to achieve such supramolecular polymers is by the attachment of appropriate supramolecular motifs onto the ends of a core unit. The backbones of the resulting self-assembled polymeric systems will, therefore, contain noncovalent bonds, in addition to covalent bonds, and these collectively impart reversibility upon the system (i.e., a dynamic degree of polymerization) and temperature sensitivity. This behavior, in turn, offers the potential to develop polymeric materials in which the melt viscosity at elevated temperatures is more akin to a monomeric-like state, and thus allows for the utilization of mild processing conditions. One

interesting opportunity offered by such systems is the ability to self-assemble functional units into processable polymeric materials, which, for example, exhibit attractive electronic and/or optical properties.[2] The properties of such noncovalently bound aggregates have a strong dependence not only on their functional core components, but also on the nature (stability and dynamics) of the supramolecular motifs that control the self-assembly process. In addition, if the supramolecular motif used in the assembly of the polymer is asymmetric (i.e., it consists of two different complementary units), then the supramolecular polymer will be formed only in the presence of both of these complementary units. For example, a heteroditopic monomer, in which both complementary units are placed on the same molecule, will result in a self-assembling $(A–B)_n$ polymer (Figure 1a). However, homoditopic monomers, which have only one of the complementary units placed on each monomer (e.g., A–A or B–B), will exhibit polymer-like properties only upon mixing of the two corresponding monomers (Figure 1b). Therefore, in this case there exists the potential that the supramolecular polymers formed will feature new functional properties that are not exhibited by the individual monomers. An example of such a supramolecular-aided function is the growing area of supramolecular liquid-crystalline materials.[3–5] In such systems, molecular-shape anisotropy is important for the formation of a liquid-crystalline (LC) phase. For example, rigid and semirigid molecules that have a high aspect ratio often exhibit liquid-crystalline behavior. Therefore, the self-assembly of small (semi)rigid units into a larger linear array, with

[a] Dr. S. Sivakova, C. J. Campo, Prof. Dr. P. T. Mather,
Prof. Dr. S. J. Rowan
Department of Macromolecular Science and Engineering
Case Western Reserve University
2100 Adelbert Road, Cleveland, OH 44106–7202 (USA)
Fax: (+1)216-368-4202
E-mail: stuart.rowan@case.edu

[b] Dr. J. Wu
Department of Chemical Engineering
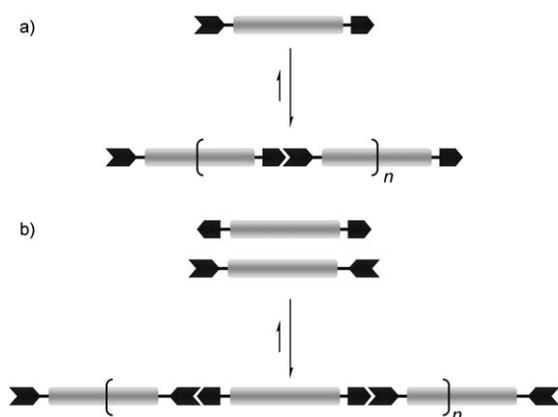University of Connecticut, Storrs, Connecticut (USA)

Figure 1. Schematic representation of two different types of supramolecular polymers that are formed by the association of monomers with complementary end-groups. a) Self-assembly of a heteroditopic monomer to yield an (AB)$_n$ supramolecular polymer, b) self-assembly of two complementary homoditopic monomers to yield an (AA–BB)$_n$ supramolecular polymer. The dynamic nature of these polymers allows them to break and recombine in response to changes in the environment.

a high axial ratio, can result in the appearance of a liquid-crystalline phase.[6–9] The induction of an LC phase in such a case is a macroscopic expression of the molecular recognition designed into the molecules. Furthermore, the formation of such an LC phase, with its long-range order, will aid in the formation of higher-molecular-weight aggregates.[10,11]

Our investigations in this field have, in part, focused on the use of nucleobase-pair interactions to control the self-assembly of fluorescent, low-molecular-weight monomers into liquid-crystalline polymeric architectures.[12] The utilization of the nucleobase interactions in supramolecular chemistry offers the opportunity to prepare precise self-assembled architectures,[13] and allows for the exploitation of different units, all of which offer various binding motifs.[14] We, and others, have shown that the placement of a single nucleobase at either end of a chain results in dramatic changes in material properties.[12,15–17] To this end, we have designed homoditopic monomers (Figure 2) in which the nucleobase thymine (T) and the nucleobase derivative N^6-(4-methoxybenzoyl)adenine (A^{An}) are substituted on both ends of an alkoxy-substituted bis(phenylethynyl)benzene core (B^{P}1aB^P and B^{P}1bB^P, B^P = nucleobase derivative). Thus, this system
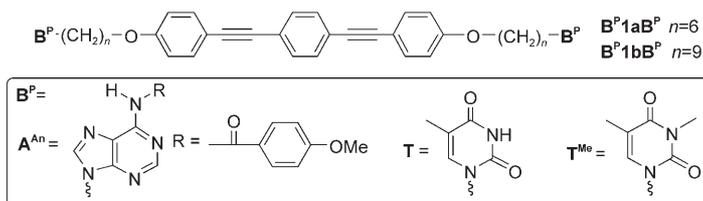

Figure 2. Structures of the homoditopic (A–A, B–B) nucleobase-terminated bis(phenylethynyl)benzene monomers (B^{P}1aB^P and B^{P}1bB^P). B^P = nucleobase derivative.

should exhibit polymer-like properties only upon mixing of the complementary monomers. Another possible design involves a heteroditopic monomer, in which both complementary units are placed on the same core, resulting in a self-assembling (AB)$_n$ polymer. This manuscript will focus on (AA–BB)$_n$ systems, and studies on a related (AB)$_n$ material will be published elsewhere.

Results and Discussion

To effectively utilize nucleobase binding motifs in the self-assembly of supramolecular liquid-crystalline polymers, it is important to consider the nature of the nucleobase interactions. Although nucleobases constrained within DNA sequences are some of the most controllable supramolecular motifs, the individual nucleobases are less predictable.[14] For example, the purines (adenine and guanine) are able to bind through two different binding sites (Watson–Crick and Hoogsteen),[18] and as a result can form multicomponent complexes. In addition, the individual nucleobases can homodimerize to form even more diverse structures, as in the case of guanine, which can form linear tapes, sheets, ribbons, and macrocycles.[19] Thus, the utilization of nucleobases beyond the constraints of a DNA backbone may require special modifications to enhance the level of predictability of the system. To this end, we investigated the binding capability of N^6-anisoyladenine with thymine.

Protection of the adenine moiety by N^6-anisoyl effectively reduces the number of possible thymine binding sites, thus preventing the formation of 2:1 T$_2$:A complexes. Consequently, the possibility of hydrogen-bond-mediated branching/crosslinking during the self-assembly process is reduced. With this in mind, we investigated the effect that such a modification has on the interaction between N^6-anisoyladenine and thymine.[20] Two model compounds, 1-dodecylthymine (dodecyl-T) and N^6-anisoyl-9-dodecyladenine (dodecyl-A^{An}), were prepared and investigated. NMR titration experiments (in CDCl$_3$), in which the shift of the N^6-H on the adenine was monitored, allowed the binding constant between these two model compounds to be estimated at around 22 M^{-1}, confirming that A^{An} and T do indeed interact with each other through hydrogen bonds. However, this indicates a significant reduction in the strength of the interaction between these two nucleobase moieties compared to the case of unprotected adenine ($K_{A–T} = 100$ M^{-1} in CDCl$_3$).[21] Nuclear Overhauser effect (NOE) experiments were carried out by utilizing a 0.1 M solution of 1:1 dodecyl-T:dodecyl-A^{An} in CDCl$_3$ to determine through which of the two purine binding sites (i.e., Hoogsteen or Watson–Crick) the modified adenine interacts with thymine. Irradiation of the dodecyl-T NH proton resulted in NOE to both the H^8 and H^2 protons of the adenine, in a 2:1 ratio. As a consequence of the limitations of this technique, direct correlations cannot be made; however, the results suggest that thymine does have a preference for the Hoogsteen face of the modified adenine, at least in solution.[20,22]

Pure homoditopic compound properties: Having demonstrated the existence of a hydrogen-bond-mediated interaction between thymine and N^6-anisoyladenine, we next studied how the placement of these supramolecular binding units affected low-molecular-weight, mesogenic core molecules. To this end, a series of nucleobase-terminated mesogenic molecules were prepared. Attention was focused on systems that were based on the alkoxy-substituted bis(phenylethynyl)benzene core unit. This fluorescent mesogen with pendant octyloxy chains (and no nucleobases attached) has been shown to display both nematic (N) and smectic (S) phases with the following thermal transition temperatures on heating (°C): K 128.3 S_1 167 S_2 182 N 218 I.[23] The symmetry of this core unit allows quick and easy access to a series of homoditopic monomers and the conjugated nature of the mesogen should impart fluorescent properties upon the resulting materials.

Scheme 1 shows the general synthetic protocol used to access a range of these homoditopic monomers, in which thymine (**T**), methylthymine (**T^{Me}**), or N^6-anisoyladenine (**A^{An}**) was placed on both ends of either a hexyloxy or nonyloxy-substituted bis(4-alkoxyphenylethynyl)-benzene unit. The first step in the synthesis of these nucleobase-terminated monomers was the reaction of p-iodophenol (**2**) with excess 1,6-dibromohexane or 1,9-dibromononane and K_2CO_3 to yield either **3a** or **3b** in 57 and 31% yield, respectively. The synthesis of **B^P4a**, in which **B^P** = **A^{An}** or **T**, was achieved in moderate yields (20–48%) by reacting **3a**, under basic conditions in DMF, with either **A^{An}** or **T**, respectively. By using a similar protocol, **B^P4b** was prepared from **3b**. Finally, the appropriate **B^P4a** (or **B^P4b**) compound was coupled to 1,4-diethynylbenzene under palladium-catalyzed Sonogashira conditions in toluene/diisopropylamine, resulting in the desired nucleobase-terminated supramolecular monomers **B^P1aB^P** (or **B^P1bB^P**) in moderate to good yield (50–82%). Synthesis of the methylated **T^{Me}1aT^{Me}** monomer involved the reaction of **T4a** with methyl iodide in K_2CO_3/DMF to yield **T^{Me}4a** in 88% yield. **T^{Me}4a** was then coupled to 1,4-diethynylbenzene in a similar manner as before, yielding the desired monomer in 75% yield. Structures of all the monomers were confirmed by both ^{1}H NMR spectroscopy and MALDI-TOF mass spectrometry.

The effect of nucleobase attachment onto the alkoxy-substituted bis(phenylethynyl)benzene core: Not surprisingly, derivatization of the ends of the alkoxy-substituted bis(phenylethynyl)benzene cores with thymine units results in a significant reduction of the temperature range in which these materials exhibit liquid-crystalline behavior, primarily through a dramatic increase in the primary melting temperature

(Figure 3). Liquid-crystallinity is observed for only a narrow temperature range above T_m, specifically 205–214°C for **T1aT** and 206–215°C for **T1bT**. **T^{Me}1aT^{Me}** also displays a liquid-crystalline phase over a narrow temperature range, but at much lower temperatures, 153–167°C, clearly revealing the importance of thymine hydrogen-bonding in determining the primary melting point. Upon cooling from a temperature greater than 214°C, **T1aT** did not exhibit any observable LC behavior, but instead crystallized at 182°C from an isotropic phase. However, both **T1bT** and **T^{Me}1aT^{Me}** do form LC phases upon cooling. Although results of differential scanning calorimetry (DSC) of **T^{Me}1aT^{Me}** show only one broad exothermic peak at 135°C (see Supporting Infor-
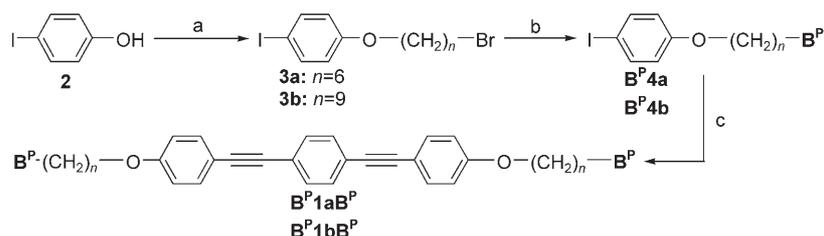
Scheme 1. Synthesis of the homoditopic (A–A, B–B) nucleobase-terminated alkoxy-substituted bis(phenylethynyl)benzene monomers. a) Br(CH₂)ₙBr [$n=6,9$], K_2CO_3, THF; b) **B^PH**, NaH, DMF; c) 1,4-diethynylbenzene, [Pd(PPh₃)₄], CuI, diisopropylamine, toluene. **B^P** = nucleobase derivative.
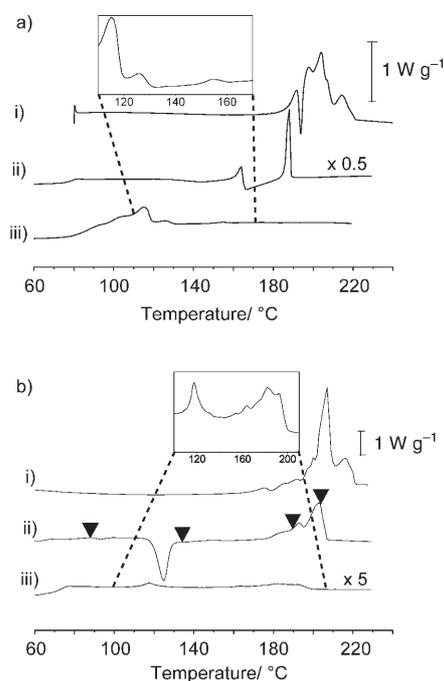

Figure 3. DSC thermograms (second heating) of the individual monomers **B^P1B^P**, in which a) six carbons or b) nine carbons separate the nucleobase from the aromatic core. Heating rate of 5°C min⁻¹ was used. The trace labeled i) corresponds to **T**-functionalized monomers, ii) to the **A^{An}**-functionalized monomers, and iii) to the 1:1 mixtures. The ▼ in b)ii) indicate the temperatures of the samples shown in the POM images in Figure 4. Endothermic heat flow is upward.

mation), results of polarising optical microscopy (POM) reveal a birefringent phase at this temperature just prior to crystallization. **T1bT**, on the other hand, exhibits a much broader LC temperature range (201–161 °C) upon cooling. Furthermore, within this LC region, a number of small exotherms are also present in the DSC thermogram. However, only subtle differences were observed in the schlieren-like textures between these transitions, and a definitive assignment of the LC phases that occur at these temperatures was not possible.

Placement of the N^6-anisoyladenine (**A^{An}**) onto the symmetrical mesogenic units also significantly alters the properties of these materials. The **A^{An}1aA^{An}** monomer displays a glass-like transition at $T_g = 82$ °C upon heating, as well as a broad crystallization exotherm at 140–180 °C before melting at 187 °C. A sharp endothermic transition is superimposed within the crystallization temperature range, occurring at 163 °C. However, the formation of a liquid-crystalline phase was not observed at any temperature for this compound. **A^{An}1bA^{An}** behaves slightly differently from **A^{An}1aA^{An}**, exhibiting a glass-like transition at $T_g = 68$ °C and two exothermic peaks, a small one at 93 °C and a much larger one at 124 °C. In addition, unlike **A^{An}1aA^{An}**, **A^{An}1bA^{An}** does exhibit a liquid-crystalline phase for the range 192–202 °C. Cooling of **A^{An}1bA^{An}** results in the formation of an LC phase at 166 °C; however, no subsequent recrystallization is observed, resulting in a "freezing in" of the texture upon formation of the glassy solid. Figure 4 shows polarized optical micrographs obtained during the second heating of **A^{An}1bA^{An}**. At 80 °C, which is above T_g, a metastable birefringent phase (Figure 4a) is observed. Upon increasing the temperature to above 130 °C, a recrystallization from this metastable LC phase occurs (Figure 4b and c). This material remains crystalline until around 190 °C (Figure 4d), before becoming isotropic above 202 °C (Figure 4e). Interestingly, the crystalliza-
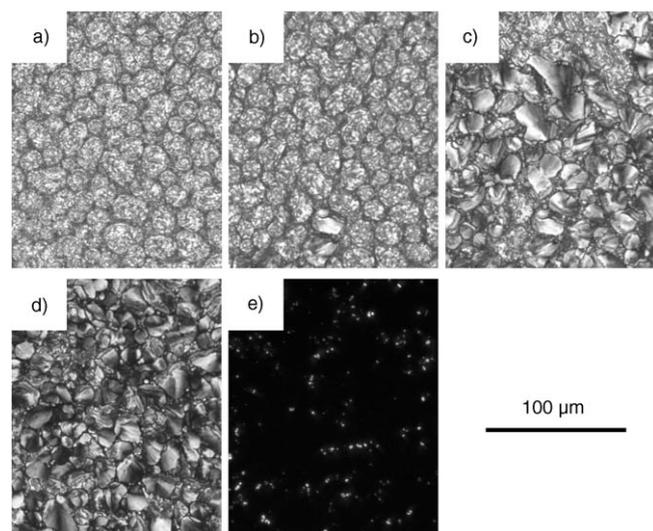
tion observed upon heating at around 130 °C does not occur on cooling, no matter how slow. Furthermore, the recrystallization occurs on heating only if the sample is first cooled to below 90 °C, suggesting that the small exotherm at 93 °C may correspond to the formation of a nucleation source for the recrystallization at elevated temperature.

Mixing complementary nucleobase-end-functionalized monomers: Melt mixing of the complementary nucleobase-terminated monomers **A^{An}1aA^{An}** and **T1aT** results in a dramatic decrease in the melting temperature, along with the concurrent appearance of a viscous birefringent phase, as shown by the results of POM (Figure 5a) for samples heated to be-
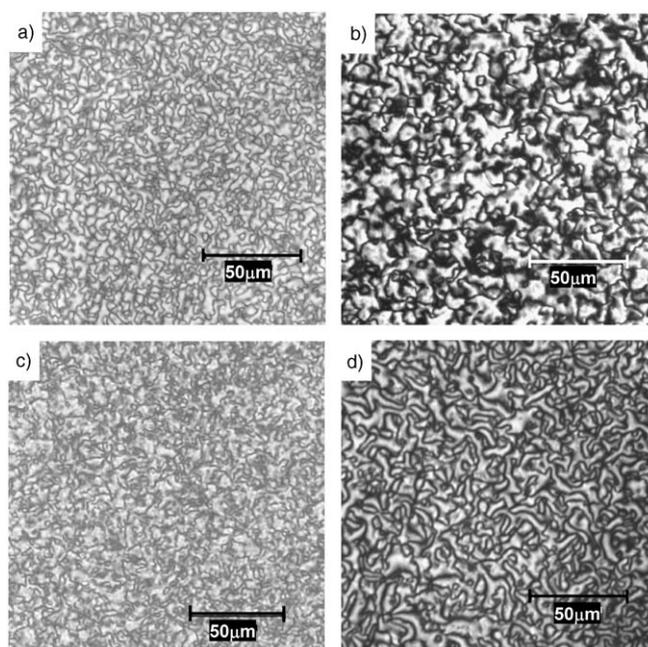

Figure 5. Polarized optical micrographs of 1:1 mixtures of a) **T1aT**:**A^{An}1aA^{An}** at 135 °C, b) **T1bT**:**A^{An}1bA^{An}** at 145 °C, c) **T1bT**:**A^{An}1aA^{An}** at 125 °C, and d) **T1aT**:**A^{An}1bA^{An}** at 135 °C.

tween 115 and 154 °C. The appearance of the liquid-crystalline phase is bounded by endothermic peaks, as observed in the DSC thermogram (Figure 3a(iii) and inset). Above 175 °C, the material behaves as a free-flowing liquid, which becomes more viscous upon subsequent cooling to below 175 °C. At 153 °C, a viscous birefringent phase was observed, which vitrified upon cooling to below 116 °C. Notably, these phenomena are not observed upon the first heating of the sample obtained by mixing the monomers in a 1:1 ratio in either solid or solution state, but are consistently present upon subsequent heating and cooling cycles. Similar observations were made for mixing of the complementary monomers **T1bT** and **A^{An}1bA^{An}**, which contain a nine-carbon chain between the rigid core and the nucleobases. Again, the formation of a viscous birefringent phase was observed by both DSC (Figure 3b(iii)) and POM (Figure 5b) analyses,

Figure 4. Polarized optical micrographs of the second heating of **A^{An}1bA^{An}** at a) 80 °C; b) 135 °C, 0 min; c) 135 °C, 2.5 min; d) 190 °C; and e) 202 °C. Heating rate 5 °C min⁻¹.

this time with a broad temperature range spanning 117–192 °C. Furthermore, intermixing of the complementary C_6 and C_9 monomers in 1:1 ratios also resulted in the formation of viscous birefringent phases (Figure 5c and d), which were observed over a temperature range of approximately 60 °C. Notably, in some of these mixed-monomer systems, the DSC thermograms show a number of small endotherms within the liquid-crystalline region. However, these transitions are accompanied by little or no difference in liquid-crystalline texture, as seen in POM images, precluding direct assignment of the LC phases that exist between each transition. The textures observed in all the samples are best described as schlieren, which is consistent with the presence of nematic and/or some smectic phases (e.g., smectic C).[24]

As for conventional liquid crystals, the orientation of our self-assembled polymers based on complementary nucleobase monomers could be macroscopically aligned with an electric field. A mixture of **T1aT**:**A**^{An}**1aA**^{An} was brought to 132 °C, 17 °C above its solid-LC phase transition, at which a birefringent texture was observed by POM analysis (Figure 6a). An electric field was then applied to the sample,
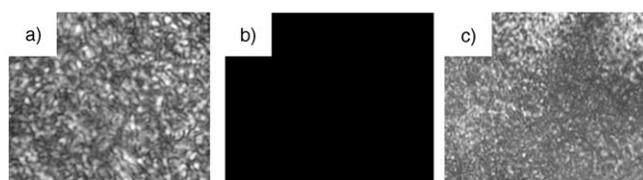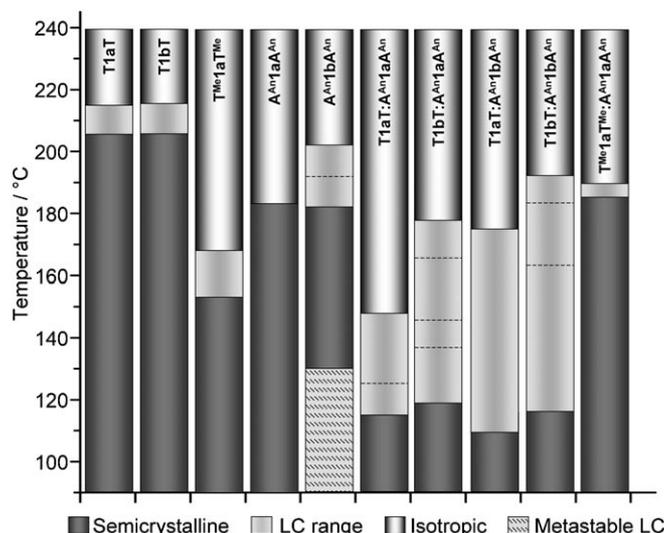

Figure 7. Summary of the phase behavior of the individual monomers and the 1:1 mixtures of complementary monomers on heating. The dotted horizontal lines correspond to additional endotherms within the liquid-crystalline range (DSC).

Figure 6. Polarized optical micrographs (magnification ×500) of a 1:1 mixture of **T1aT** and **A**^{An}**1aA**^{An} at 132 °C a) before application of an electric field, b) after application of an electric field (300 V), and c) upon removal of an electric field.

causing the LC director to align parallel to the field direction, yielding darkness under POM viewing conditions (Figure 6b), consistent with homeotropic alignment. Interestingly, upon removal of the electric field, the director relaxed and a schlieren texture was again observed, but now with a finer scale (Figure 6c). The return to a textured orientation distribution may be due to the lack of homeotropic surface treatment of the glass surfaces, which would have preserved orientation upon removal of the field. The relaxation took several seconds to occur, which is longer than expected for a small-molecule LC material. We attribute this difference to supramolecular polymerization and an associated higher viscosity.

Figure 7 summarizes the liquid-crystalline phases observed upon heating for all the materials discussed above. For all the mixed-monomer systems, it is postulated that the observed liquid-crystalline phase, which occurs over a much broader temperature range than is exhibited by the individual monomers, is a consequence of complementary nucleobase interactions that result in the formation of larger supramolecular aggregates. Scheme 2 shows a proposed model, in which the nucleobases form hydrogen bonds through the re-

verse-Hoogsteen interaction, resulting in the formation of long, linear chains. The assembly of longer linear aggregates increases the effective aspect ratio of the molecules and consequently induces conditions more favorable for LC formation and stability. Moreover, the supramolecular aggregates would have more difficulty packing into a crystalline lattice, thus lowering T_m and effectively broadening the LC window.

To understand more fully the nature of the liquid-crystal phases observed, wide angle X-ray diffraction (WAXD) studies were performed on all of the 1:1 complementary mixtures (Figure 8). The samples were prepared by solution-mixing the complementary monomers, casting into films, heating the samples to above 200 °C, and subsequently cooling at approximately 5 °C min^{-1}. Little or no crystallization was observed by POM in these samples and the LC structure that existed prior to vitrification was frozen-in upon cooling. Furthermore, a glass-like transition is observed in the DSC thermogram for all such samples; therefore, X-ray data was recorded at room temperature. The WAXD patterns obtained for all of these mixtures are consistent with the presence of a smectic phase prior to vitrification, as evidenced by a sharp, low-angle ring superposed by much broader reflections at wider angles. For the **T1aT**:**A**^{An}**1aA**^{An} mixture, in which both components have six carbon atoms between the nucleobase and the rigid mesogenic unit, the low-angle ring was characterized by a d-spacing of 37.5 Å. This distance is slightly, but significantly, less than the supramolecular polymer repeating length of 41 Å estimated from molecular modeling studies of the Hoogsteen hydrogen-bonded aggregate shown in Scheme 2. Thus, our WAXD observation implies a smectic C arrangement with mesogens tilted away from the layer normal at an angle of 24°. As expected, increasing the length of the alkyl space group from six to nine increased the smectic layer spacing to approxi-
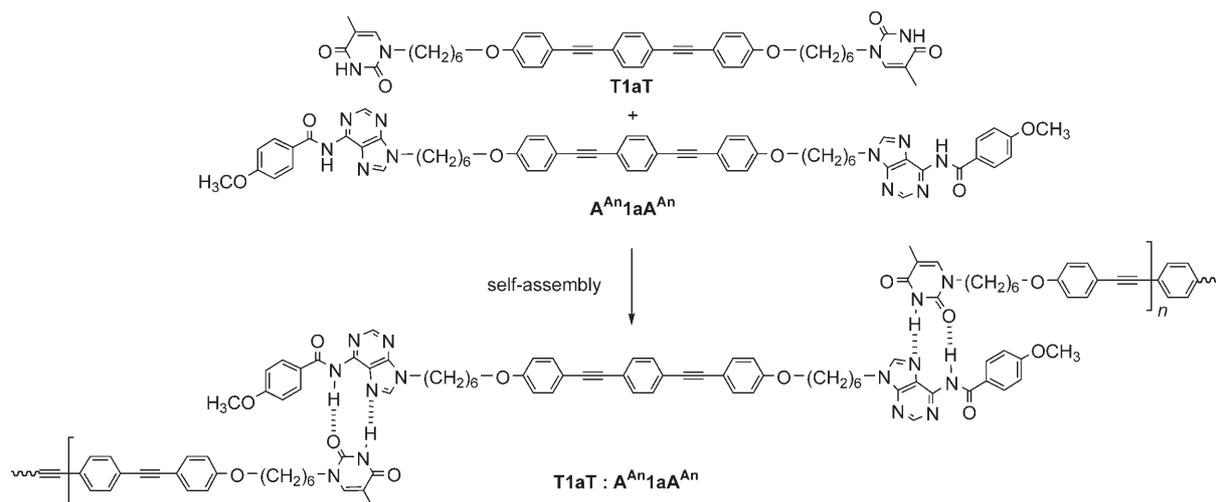
Scheme 2. Proposed nucleobase-induced, self-assembled fluorescent polymer (**T1aT**:**A^{An}1aA^{An}**).
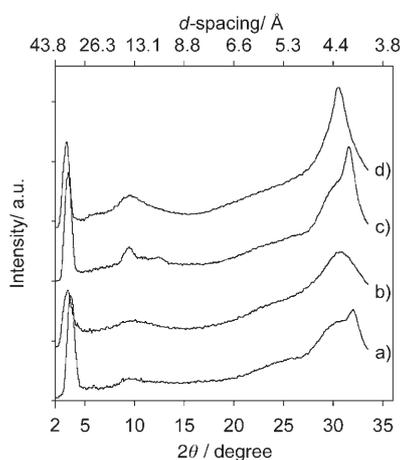

Figure 8. WAXD data obtained at RT of a) **T1aT:A^{An}1aA^{An}**, b) **T1aT:A^{An}1bA^{An}**, c) **T1bT:A^{An}1aA^{An}**, and d) **T1bT:A^{An}1bA^{An}**.

mately 40 Å for **T1bT:A^{An}1aA^{An}** and **T1aT:A^{An}1bA^{An}**, and 41.8 Å for **T1bT:A^{An}1bA^{An}**. In each case, the measured d-spacing is less than that estimated from molecular modeling (ca. 45 Å for **T1bT:A^{An}1aA^{An}** and **T1aT:A^{An}1bA^{An}**, and ca. 49 Å for **T1bT:A^{An}1bA^{An}**), suggesting that these mixtures also form a smectic C phase before vitrification, with mesogen tilt angles of 27 and 31°, respectively.

Consistent with the formation of supramolecular liquid-crystalline polymers, fibers could be obtained from the melt of the 1:1 **B^P1B^P** complementary-monomer mixtures. Figure 9a shows a POM image of one such fiber obtained from the LC phase of the **T1bT:A^{An}1bA^{An}** mixture at around 145 °C. Figure 9b shows the X-ray fiber diffraction pattern, which confirms modest molecular orientation induced by drawing. In particular, diffraction rings at d-spacings of 12 and 4.5 Å, visible in unoriented specimens (data not shown), are split into off-axis reflections, suggesting a tilted arrangement of liquid-crystalline layering. By virtue of the fluores-
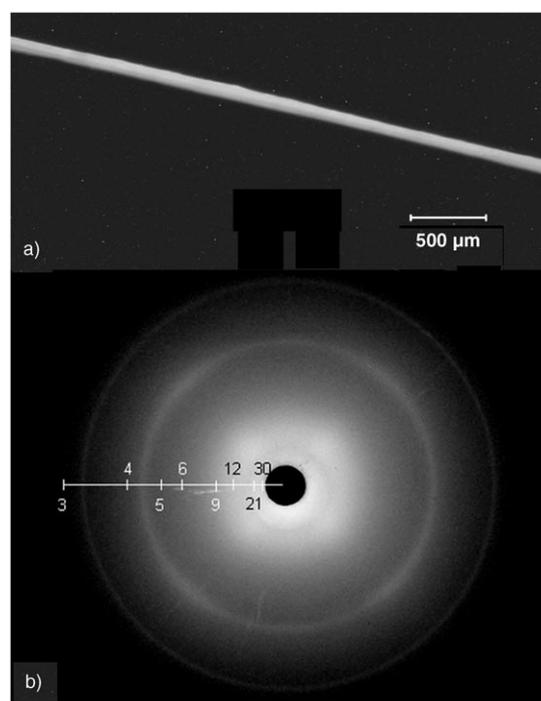

Figure 9. a) Polarized optical micrograph of a fiber pulled from the melt of a **T1bT:A^{An}1bA^{An}** mixture. b) WAXD patterns of a fiber of **T1bT:A^{An}1bA^{An}**. The calibrated d-spacings are indicated on the pattern in Angstroms. The fiber axis was vertical.

cent mesogenic core present in these monomers, the fibers obtained from the **T1bT:A^{An}1bA^{An}** mixtures are themselves fluorescent.

The effect of altering the thymine: N^6-anisoyladenine stoichiometry: If supramolecular polymers are indeed formed by the self-assembly of complementary ditopic monomers, then addition of a mono-adenine derivative, which will act as a supramolecular-chain terminator, will proportionally de-

polymerize the supramolecular chains. As a consequence, modification of the material properties towards those observed for the monomers should occur. To test this idea, dodecyl-A^{An} was added to a 1:1 mixture of **T1aT**:A^{An}**1a**A^{An}. Indeed, addition of even small amounts of dodecyl-A^{An} quickly reduced the thermal range of the observed liquid-crystalline phase. In the absence of dodecyl-A^{An}, the liquid-crystal phase spanned a broad 39 °C. However, addition of 5 % dodecyl-A^{An} resulted in significant destabilization of the LC phase, with a reduction in the LC range to only 22 °C (Figure 10). The addition of 25 % of chain terminator resulted in the complete abolition of liquid-crystalline properties. The fact that liquid-crystalline phases were still observed after addition of up to 20 % of chain terminator suggests that even relatively short oligomeric chains are sufficient to induce some liquid-crystal formation.
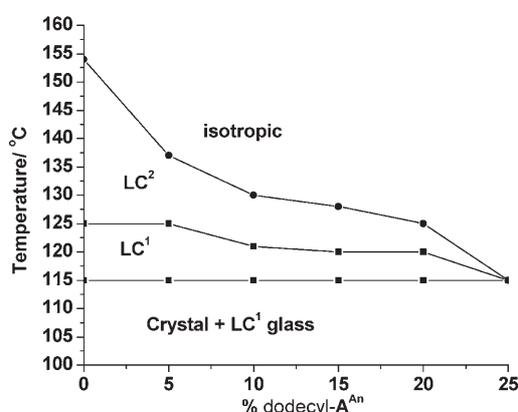

Figure 10. Phase diagram depicting the effects of monofunctional dodecyl-A^{An} on the liquid-crystalline phase of the **T1aT**:A^{An}**1a**A^{An} mixture.

Another method of altering the stoichiometry of the two binding units is to change the ratio of the two complementary monomers. To obtain the maximum degree of polymerization, an exact 1:1 molar equivalent of the complementary monomers is crucial. An excess of one of the monomers will essentially act as a chain terminator in an analogous way to the addition of the mono-adenine derivative. Therefore, we investigated the effects of different stoichiometries of **T1bT** and A^{An}**1b**A^{An} in the monomer mixtures on the stability of the liquid-crystalline phases. Interestingly, the addition of up to 50 % excess equivalents of either monomer did not result in dramatic changes, as shown by DSC analysis. For example, the addition of 1.5 equivalents of **T1bT** to 1 equivalent of A^{An}**1b**A^{An}, or vice versa, resulted in only slight shifts relative to the 1:1 mixture in the T_g, the T_m, as well as in the clearing transition. These results are qualitatively consistent with those obtained by addition of a monofunctional chain-terminator, again suggesting that only low-molecular-weight aggregates are required to induce and stabilize liquid-crystal phase formation. However, it should be noted that altering the stoichiometry of the complementary nucleobases, either by addition of a monofunctionalized compound or by changing the ratio of the monomer units, does reduce the solid- and liquid-state mechanical properties of these materials. For example, fibers cannot be obtained from the melt of materials that do not have a 1:1 stoichiometry of the two nucleobases, which is in line with the formation of only low-molecular-weight aggregates in these systems. We note that conventional solution-based analyses for molecular-weight determination cannot be applied to these materials; therefore, only melt or solid-state properties can be used to infer effective chain length.

Disruption of the hydrogen-bonding motif: The proposed self-assembly model outlined in Scheme 2 assumes that hydrogen bonding plays an important role in the supramolecular polymerization of these molecules. To test this model, specifically for the adenine–thymine base-pair, the N^3-methylated thymine monomer **T^{Me}1aT^{Me}** was prepared and investigated. The placement of a methyl group on the nitrogen at the 3 position of the thymine effectively disrupts the hydrogen bonding between these complementary nucleobase moieties. As discussed previously, **T^{Me}1aT^{Me}** itself has a lower melting temperature ($T_m = 153$ °C) than the **T1aT** monomer ($T_m = 205$ °C), but does exhibit a narrow liquid-crystalline phase (153–167 °C). An equimolar mixture of **T^{Me}1aT^{Me}** with A^{An}**1a**A^{An} produces a material that exhibits three endotherms, as shown by the results of DSC, at 100, 133, and 182 °C. Although an LC phase is observed for this mixture, the LC region occurs at much higher temperatures than for the hydrogen-bonded mixtures and over a narrower temperature range (185–190 °C). Furthermore, this sample is less homogenous than the hydrogen-bonded materials and, from the results of both POM and DSC, it appears that there are two melting points (ca. 130 °C and ca. 180 °C), consistent with the presence of two separate crystalline regions. From POM observations there appears to be no melting at 100 °C, suggesting that this endotherm in the DSC thermogram corresponds to a solid-state transition. In addition, the LC phase that is observed for this mixture is a free-flowing liquid from which no fibers could be obtained, in stark contrast to the highly viscous liquid-crystal phases formed by the **T1aT**:A^{An}**1a**A^{An} mixtures.

To further compare the nature of the hydrogen-bond interactions in these materials, infrared spectroscopy of the annealed films (ca. 200 °C) on CaF_2 disks was carried out. Figure 11a shows the FTIR spectrum of the neat materials **T^{Me}1aT^{Me}** and A^{An}**1a**A^{An}. Comparison of the spectra obtained from **T1aT**:A^{An}**1a**A^{An} and **T^{Me}1aT^{Me}**:A^{An}**1a**A^{An} (Figure 11b) reveals vast differences in both the NH and carbonyl stretching regions. The **T1aT**:A^{An}**1a**A^{An} mixture exhibits a broad shoulder at 2800 cm^{-1}, indicative of the presence of medium-strength hydrogen bonding.[25] In addition, two NH stretching vibrations are observed: one at 3183 cm^{-1}, consistent with the presence of hydrogen-bonded NH groups, and a small peak at 3413 cm^{-1}, consistent with the presence of some free NH groups.[26] Furthermore, there is one very broad carbonyl peak spanning from 1718–1658 cm^{-1}, suggesting the involvement of the carbonyl units in hydrogen
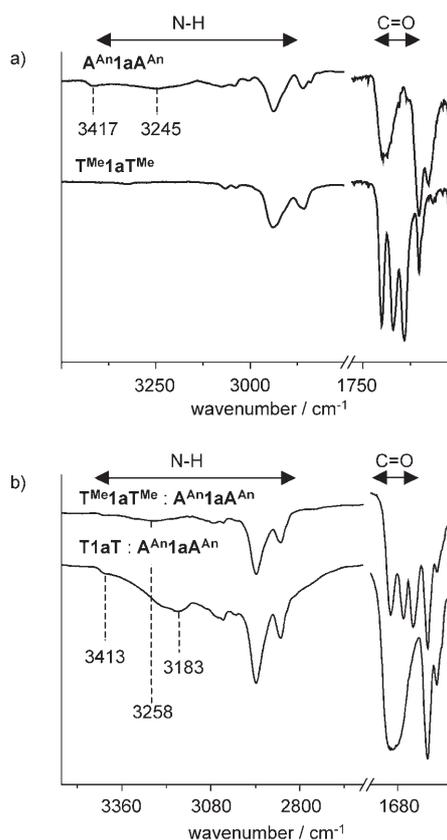
Figure 11. IR spectra of the NH stretching region and the carbonyl region of a) $T^{Me}1aT^{Me}$ vs $A^{An}1aA^{An}$ and b) $T1aT:A^{An}1aA^{An}$ vs $T^{Me}1aT^{Me}:A^{An}1aA^{An}$ mixtures.

bonding. This data indicates that in the solid-state, **T1aT**: **$A^{An}1aA^{An}$** does indeed form hydrogen-bonded supramolecular aggregates. The **$T^{Me}1aT^{Me}:A^{An}1aA^{An}$** mixture, on the other hand, shows no broad shoulder at 2800 cm⁻¹ and a very weak NH stretching peak centered at 3258 cm⁻¹. This stretching results from the NH on the **$A^{An}1aA^{An}$** monomer, which has a wavenumber of 3245 cm⁻¹ in neat **$A^{An}1aA^{An}$** (Figure 11a). In addition, the carbonyl stretching region shows multiple, sharp carbonyl peaks. Peaks at 1697 and 1667 cm⁻¹ correspond to the two carbonyl groups found in **$T^{Me}1aT^{Me}$**, with presumably the carbonyl peak from **$A^{An}1aA^{An}$** overlapping these peaks. The sharpness of the peaks suggests that each carbonyl moiety exists in its own distinctive environment and thus unlikely to be involved in hydrogen bonding. This data is consistent with there being no significant hydrogen-bond interactions between the two components in this material.

Conclusion

We have shown that the binding motif consisting of thymine and N^6-(4-methoxybenzoyl)adenine can be used to control the aggregation of symmetrically-substituted alkoxy-bis(phenylethynyl)benzene units, resulting in A–A/B–B-type poly-

meric species that form relatively stable LC phases. Concurrent with the formation of the viscous birefringent phases, the materials also demonstrate the ability to form oriented, fluorescent fibers. Thus, we have utilized the functionality of the core unit to aid LC formation and to impart fluorescent behavior, in conjunction with the self-assembling capability of the nucleobases, which not only aids LC formation, but also imparts polymer-like properties, such as fiber formation, to the material. Further investigations are underway to examine the possibility of using such weak noncovalent binding groups to obtain polymeric materials that show high thermal sensitivity. Such materials will exhibit very low melt-viscosities and could open the door to facile processing of functional (conjugated) polymers, cheaper recycling of plastics, or even thermally repairable materials.[27]

Experimental Section

Materials: The N^6-(4-methoxybenzoyl)adenine was synthesized according to literature procedures.[28] All reagents and solvents were purchased from Aldrich. Reagents were used without further purification. Solvents were distilled from suitable drying agents.

Characterization: ¹H and ¹³C NMR spectra were recorded by using either a Varian Gemini 200 MHz, a Varian 300 MHz, or a Varian 600 MHz NMR spectrometer. Differential scanning calorimetry (DSC) experiments were performed by using a Pyris 1 DSC (Perkin–Elmer) under flowing N₂ at a heating rate of 5°C min⁻¹. Polarising optical microscopy (POM) studies were performed by using an Olympus BX51 microscope equipped with crossed polarizers, an HCS 402 hot stage from Instec, and a digital color CCD camera (SPOT Insight Firewire Color Mosaic). Images were acquired from the CCD camera at selected times and/or temperatures by using SPOT software (Diagnostic Instruments). Spatial dimensions were calibrated by using a stage micrometer with 10 μm line spacing. The samples used for POM analysis were sandwiched between two glass coverslips. The temperature ramping rates were chosen to be consistent with DSC experiments for comparison purposes. The hot stage was equipped with a liquid nitrogen LN2-P 110 VAC cooling unit from Instec for the accurate control of sample temperature, either isothermally or during heating and cooling runs. FTIR measurements were performed by using a Biorad Excalibur Series FTS3000MX spectrometer. Molecular weights of materials were measured by mass spectrometry on a Bruker BIFLEX III MALDI-TOF mass spectrometer (matrix: α-cyano-4-hydroxycinnamic acid). Two-dimensional X-ray data of fibers drawn in the vertical direction was obtained by using a Philips PW1830 generator with Ni-filtered Cu$_{K\alpha}$ radiation, a calibrated sample-detector distance of 5.45 cm, and image plates (Model #FDL-UR-V, Fuji Photo Film) with 25 μm pixel size. Wide angle X-ray diffraction measurements on cast films were recorded at the University of Connecticut by using a GADDS-4 (Bruker AXS); X-ray source: Cr ($\lambda=2.291$ Å); experimental conditions: 40 kV, 40 mA, RT.

Binding studies: The binding studies were performed by using deuterated chloroform predried with potassium carbonate. A mixture of dodecyl-**T** (20 mм) and dodecyl-**A^{An}** (5 mм) was titrated to a stock solution of dodecyl-**A^{An}** (5 mм) so that the concentration of dodecyl-**T** varied from 1 to 16 mм. The shift of the hydrogen on the N^6 position of the adenine was monitored with respect to chloroform and the data was fitted to the equation for a 1:1 binding.

¹H NMR NOE experiments: Experiments were performed by using a Varian 600 MHz NMR spectrometer at −30°C in CDCl₃, pulse width: 39.3°, mixing time: 0 sec, acquisition time: 1.5 s. Concentration of both dodecyl-**T** and dodecyl-A^{An} was 100 mм.

Field-induced alignment of LC phases: The material was sandwiched between two indium tin oxide-coated slides. Two 2 μm flexible spacers were

used to separate the glass slides. Aluminum electrodes were attached to the cell and the whole assembly was wrapped in Teflon tape to prevent short circuiting. The electrodes were then connected to a high-voltage DC power supply (Bertan Associates, Model 2.5). The entire cell was placed inside a heating stage (Mettler FP85 Hot Stage) and the sample temperature was elevated to 132 °C. Once this temperature was reached, a potential difference of 300 V (150 V μm⁻¹) was applied across the sample. Results of field application were observed by POM and recorded by using a microscope-mounted digital camera.

General procedure for preparing 3a and 3b

A suspension of potassium carbonate (K_2CO_3) (8.00 g, 57.9 mmol) and DMF (30 mL) was purged with argon for 15 min and heated to 70 °C, at which time 4-iodophenol (**2**) (5.00 g, 23.0 mmol) was added. The appropriate alkyl bromide (46.2 mmol) was then added quickly by means of a syringe, and the suspension was stirred at 70 °C under argon sparging for 4 h.

4-(1-Hexyloxy-6-bromo)-1-iodobenzene (3a): The reaction was conducted according to the general procedure described above, using 1,6-dibromo-hexane (7.1 mL, 46.2 mmol). The solvent was evaporated and the residue was dissolved in methylene chloride (CH_2Cl_2). The organic phase was washed with water twice and then evaporated, and the residue was left to dry in a vacuum oven overnight. Column chromatography (silica gel; 99:1 hexane/toluene) of the resulting crude product afforded pure **3a** as a white solid (5.05 g, 57%). M.p. 57 °C; ¹H NMR (CDCl₃, 200 MHz): $\delta =$ 7.55 (d, 2H; ArH), 6.67 (d, 2H; ArH), 3.93 (t, 2H; OCH₂), 3.43 (t, 2H; BrCH₂), 1.91 (t, 2H; OCH₂CH₂), 1.81 (t, 2H; BrCH₂CH₂), 1.50 ppm (m, 4H; 2×alkyl CH₂); ¹³C NMR (CDCl₃, 75 MHz): $\delta =$ 159.2, 138.4, 117.2, 82.8, 68.1, 34.0, 32.9, 29.3, 28.2, 25.6 ppm; MS (MALDI-TOF): m/z: 382 $[M+H]^+$.

4-(1-Nonyloxy-6-bromo)-1-iodobenzene (3b): The reaction was conducted according to the general procedure described above, using 1,9-dibromo-nonane (8.33 mL, 46.2 mmol). The solvent was evaporated and the residue was dissolved in CH_2Cl_2. The organic phase was washed with water twice, separated, and reduced in volume. The unwanted bis-functional-ized alkane was precipitated out with methanol. The soluble fraction was then evaporated and the residue was dried in a vacuum oven overnight. Column chromatography (silica gel; hexane) of the resulting crude product afforded pure **3b** as a white solid (3.03 g, 31%). M.p. 56 °C; $R_f = 0.39$ (hexane); ¹H NMR (CDCl₃, 200 MHz): $\delta =$ 7.55 (d, 2H; ArH), 6.67 (d, 2H; ArH), 3.93 (t, 2H; OCH₂), 3.43 (t, 2H; BrCH₂), 1.94–1.71 (m, 4H; OCH₂CH₂ and BrCH₂CH₂), 1.35 ppm (m, 10H; 5×alkyl CH₂); ¹³C NMR (CDCl₃, 75 MHz): $\delta =$ 159.3, 138.4, 117.2, 82.7, 68.3, 34.3, 33.1, 29.6, 29.5, 29.4, 28.9, 28.4, 26.2 ppm; MS (MALDI-TOF): m/z: 426 $[M+H]^+$.

General procedure for preparing T4a and T4b

Thymine (4.00 g, 31.7 mmol) was suspended in DMF (30 mL) and al-lowed to stir while sodium hydride (NaH) (0.41 g, 17.3 mmol) was added in portions. The mixture was stirred for a further 0.5 h, then **3a** or **3b** (15.6 mmol) was added in a single aliquot, and the mixture was left to stir overnight at 100 °C. The resulting mixture was neutralized with 2 mL of acetic acid and the solvent was evaporated. The residue was dissolved in CH_2Cl_2 and washed once with water. The organic layer was separated and any precipitates formed were filtered off. The CH_2Cl_2-soluble frac-tion was then evaporated and the residue was dried overnight in a vacuum oven.

4-(1-Hexyloxy-6-thymine)-1-iodobenzene (T4a): The reaction was con-ducted according to the general procedure described above, using **3a** (5.94 g, 15.6 mmol). Column chromatography (silica gel; 99:1 CH_2Cl_2/MeOH) of the resulting crude product afforded pure **T4a** as a white solid (1.33 g, 20%). M.p. 139 °C; $R_f = 0.5$ (99:1 CH_2Cl_2/MeOH); ¹H NMR (CDCl₃, 200 MHz): $\delta =$ 9.11 (s, 1H; NH), 7.55 (d, 2H; ArH), 6.97 (s, 1H; T-CH), 6.67 (d, 2H; ArH), 3.92 (t, 2H; OCH₂), 3.71 (t, 2H; NCH₂), 1.92 (s, 3H; T-CH₃), 1.84–1.65 (m, 4H; OCH₂CH₂ and NCH₂CH₂), 1.61–1.35 ppm (m, 4H; 2×alkyl CH₂); ¹³C NMR (CDCl₃, 50 MHz): $\delta =$ 166.1, 160.4, 152.6, 141.9, 139.7, 118.4, 112.2, 84.1, 69.3, 49.9, 30.6, 30.5, 27.7, 27.2, 13.9 ppm; MS (MALDI-TOF): m/z: 429 $[M+H]^+$.

4-(1-Nonyloxy-6-thymine)-1-iodobenzene (T4b): The reaction was con-ducted according to the general procedure described above, using **3b**

(6.63 g, 15.6 mmol). Column chromatography (silica gel; 99:1 CH_2Cl_2/MeOH) of the resulting crude product afforded pure **T4b** as a white solid (3.52 g, 48%). M.p. 98 °C; $R_f = 0.54$ (95:5 CH_2Cl_2/MeOH); ¹H NMR (CDCl₃, 200 MHz): $\delta =$ 8.76 (s, 1H; NH), 7.55 (d, 2H; ArH), 6.97 (s, 1H; T-CH), 6.67 (d, 2H; ArH), 3.90 (t, 2H; OCH₂), 3.68 (t, 2H; NCH₂), 1.92 (s, 3H; T-CH₃), 1.84–1.65 (m, 4H; OCH₂CH₂ and Br-CH₂CH₂), 1.62–1.35 ppm (m, 10H; 5×alkyl CH₂); ¹³C NMR (CDCl₃, 75 MHz): $\delta =$ 164.3, 159.2, 150.9, 140.6, 138.4, 117.2, 110.8, 103.6, 82.7, 68.3, 48.8, 29.6, 29.5, 29.3, 26.7, 26.2, 12.6 ppm; MS (MALDI-TOF): m/z: 471 $[M+H]^+$.

General procedure for preparing A^An4a and A^An4b

N^6-(4-Methoxybenzoyl)adenine (1.83 g, 6.80 mmol) was suspended in DMF (20 mL) and allowed to stir while NaH (0.26 g, 10.9 mmol) was added in portions. The resulting mixture was stirred for a further 0.5 h, then **3a** or **3b** (5.22 mmol) was added in a single aliquot, and the reaction mixture was left to stir for 24 h at 30 °C. The reaction was quenched by a small amount of methanol and the solvent was evaporated. The residue was dissolved in CH_2Cl_2 and washed once with water. The organic layer was separated and any precipitates formed were filtered off. The CH_2Cl_2 was then evaporated.

4-(1-Hexyloxy-6-(N^6-(4-methoxybenzoyl)adenine)-1-iodobenzene (A^An4a): The reaction was conducted according to the general procedure described above, using **3a** (1.98 g, 5.22 mmol). The residue was dissolved in a small amount of CH_2Cl_2 and excess hexane was added, resulting in the formation of a white crystalline product that was filtered off and dried under vacuum overnight. Column chromatography (silica gel; 97:3 CH_2Cl_2/MeOH) of the resulting crude product afforded pure **A^An4a** as a white solid (1.30 g, 43.8%). M.p. 126 °C; $R_f = 0.62$ (95:5 CH_2Cl_2/MeOH); ¹H NMR (CDCl₃, 200 MHz): $\delta =$ 8.9 (s, 1H; NH), 8.79 (s, 1H; adenine H-8), 8.00 (s, 1H; adenine H-2), 8.02 (d, 2H; anis-ArH), 7.55 (d, 2H; ArH), 7.00 (d, 2H; anis-ArH), 6.65 (d, 2H; ArH), 4.30 (t, 2H; NCH₂), 3.93 (t, 2H; OCH₂), 3.90 (s, 3H; OCH₃), 2.05–1.88 (m, 2H; NCH₂CH₂), 1.88–1.65 (m, 2H; OCH₂CH₂), 1.65–1.35 ppm (m, 4H; 2×alkyl CH₂); ¹³C NMR (CDCl₃, 50 MHz): $\delta =$ 165.8, 164.7, 160.3, 154.0, 153.6, 151.3, 144.3, 139.7, 131.6, 127.4, 124.6, 118.4, 115.5, 84.1, 69.2, 57.1, 45.6, 31.5, 30.5, 27.9, 27.1 ppm; MS (MALDI-TOF): m/z: 572 $[M+]^+$.

4-(1-Nonyloxy-6-(N^6-(4-methoxybenzoyl)adenine)-1-iodobenzene (A^An4b): The reaction was conducted according to the general procedure described above, using **3b** (2.21 g, 5.22 mmol) and afforded a yellow oil after removal of the CH_2Cl_2. Column chromatography (silica gel; 90:10 CH_2Cl_2/MeCN) of the resulting crude product afforded pure **A^An4b** as a white solid (1.37 g, 43%). M.p. 138 °C; $R_f = 0.52$ (80:20 CH_2Cl_2/MeCN); ¹H NMR (CDCl₃, 200 MHz): $\delta =$ 8.95 (s, 1H; NH), 8.79 (s, 1H; adenine H-2), 8.00 (s, 1H; adenine H-8), 8.02 (d, 2H; anis-ArH), 7.55 (d, 2H; ArH), 7.00 (d, 2H; anis-ArH), 6.65 (d, 2H; ArH), 4.30 (t, 2H; NCH₂), 3.93 (t, 2H; OCH₂), 3.90 (s, 3H; OCH₃), 2.05–1.88 (m, 2H; NCH₂CH₂), 1.88–1.65 (m, 2H; OCH₂CH₂), 1.55–1.25 ppm (m, 10H; internal CH₂); ¹³C NMR (CDCl₃, 75 MHz): $\delta =$ 164.4, 163.4, 159.2, 152.7, 152.4, 149.9, 143.1, 138.4, 130.3, 126.1, 123.4, 117.2, 114.3, 82.7, 68.3, 55.8, 44.4, 30.3, 29.6, 29.5, 29.4, 29.2, 26.9, 26.2 ppm; MS (MALDI-TOF): m/z: 614 $[M+H]^+$.

General procedure for preparing B^P1aB^P and B^P1bB^P (B^P=T and A^An)

In a glove box, 1,4-diethynylbenzene (0.25 g, 1.98 mmol), **B^P4** (4.36 mmol), [Pd(PPh₃)₄] (24.9 mg, 2.16×10^{-5} mol), and CuI (4.20 mg, 2.16×10^{-5} mol) were added to a 3:1 v/v mixture of toluene/diisopropyl-amine (90 mL). After the mixture was heated to 75 °C, a precipitate start-ed to appear. The mixture was stirred for 18 h at 75 °C under an argon at-mosphere. The resulting strongly luminescent suspension was subsequent-ly dropped slowly into an excess of MeOH (~200 mL), and the precipi-tate was collected and dried under vacuum.

4-(1-Hexyloxy-6-(thymine))-1-bis(phenylethynyl)benzene (T1aT): The re-action was conducted according to the general procedure described above, using **T4a** (1.86 g, 4.36 mmol) to afford a yellow solid. Column chromatography (silica gel; 95:5 CH_2Cl_2/MeOH) of the resulting crude product afforded pure **T1aT** as a yellow solid (1.17 g, 82%). ¹H NMR (CDCl₃, 600 MHz): $\delta =$ 8.76 (s, 2H; NH), 7.47 (s, 4H; ArH), 7.46 (d, 4H; ArH), 6.97 (s, 2H; T-CH), 6.86 (d, 4H; ArH), 3.98 (t, 4H; OCH₂), 3.71 (t, 4H; NCH₂), 1.93 (s, 6H; T-CH₃), 1.84–1.65 (m, 8H; OCH₂CH₂ and NCH₂CH₂), 1.60–1.35 ppm (m, 8H; 4×alkyl CH₂); ¹³C NMR (DMSO at

70 °C, 75 MHz): 164.9, 159.9, 151.6, 141.9, 133.7, 132.0, 123.4, 115.7, 114.8, 109.2, 92.3, 88.4, 68.5, 47.9, 29.2, 29.1, 26.3, 25.9, 12.5 ppm; FTIR (annealed film on CaF$_2$): $\tilde{\nu}$ = 3164, 3039, 2935, 2857, 2215, 1684, 1653, 1602, 1518, 1469, 1354, 1283, 1244, 1173 cm^{-1}; UV: λ_{max} = 274, 332, 353, 383 nm; photoluminescence (excitation at 340 nm, CHCl$_3$): 366, 384; DSC (T_m = 215 °C); MS (MALDI-TOF): m/z: 726 [M^+].

4-(1-Nonyloxy-6-(thymine))-1-bis(phenylethynyl)benzene (**T1bT**): The reaction was conducted according to the general procedure described above, using **T4b** (2.05 g, 4.36 mmol), and afforded a yellow solid. Column chromatography (silica gel; 100:0, 99:1, 98:2 CH$_2$Cl$_2$/MeOH) of the resulting crude product afforded pure **T1bT** as a yellow solid (1.02 g, 64 %). ^{1}H NMR (CDCl$_3$, 600 MHz): δ = 8.32 (s, 2H; NH), 7.47 (s, 4H; ArH), 7.46 (d, 4H; ArH), 6.97 (s, 2H; T-C*H*), 6.86 (d, 4H; ArH), 3.98 (t, 4H; OCH$_2$), 3.71 (t, 4H; NCH$_2$), 1.93 (s, 6H; T-C*H*$_3$), 1.84–1.65 (m, 8H; OCH$_2$C*H*$_2$ and NCH$_2$C*H*$_2$), 1.60–1.35 ppm (m, 20H; 10×alkyl CH$_2$); ^{13}C NMR (CDCl$_3$, 75 MHz): δ = 164.5, 159.6, 151.1, 140.7, 133.3, 131.6, 123.4, 115.2, 114.9, 110.8, 91.5, 88.2, 68.3, 48.8, 29.6, 29.5, 29.3, 26.6, 26.2, 12.6 ppm; FTIR (annealed film on CaF$_2$) $\tilde{\nu}$ = 3165, 3037, 2927, 2854, 2215, 1683, 1519, 1486, 1486, 1356, 1246, 1173 cm^{-1}; UV: λ_{max} = 281, 333, 353, 377 nm; photoluminescence (excitation at 340 nm, CHCl$_3$): 367, 385; DSC (T_m = 207 °C); MS (MALDI-TOF): m/z: 810 [M^+].

4-(1-Hexyloxy-6-(N^6-(4-methoxybenzoyl)adenine)-1-bis(phenylethynyl)benzene (**A^{An}1aA^{An}**): The reaction was conducted according to the general procedure described above, using **A^{An}4a** (2.49 g, 4.36 mmol), and afforded a yellow solid. Column chromatography (silica gel; 99:1, 98:2→95:5 CH$_2$Cl$_2$/MeOH) of the resulting crude product afforded pure **A^{An}1aA^{An}** as a yellow solid (1.14 g, 57 %). ^{1}H NMR (CDCl$_3$, 600 MHz): δ = 9.09 (br s, 2H; NH), 8.76 (s, 2H; adenine H-8), 8.01 (s, 2H; adenine H-2), 8.00 (d, 4H; anis-ArH), 7.44 (d, 4H; ArH), 7.43 (s, 4H; ArH), 6.98 (d, 4H; anis-ArH), 6.83 (d, 4H; ArH), 4.27 (t, 4H; NCH$_2$), 3.94 (t, 4H; OCH$_2$), 3.87 (s, 6H; anis-OCH$_3$), 2.05–1.88 (m, 4H; NCH$_2$C*H*$_2$), 1.88–1.65 (m, 4H; OCH$_2$C*H*$_2$), 1.55–1.25 ppm (m, 8H; 4×alkyl CH$_2$); ^{13}C NMR (DMSO at 70 °C, 75 MHz): δ = 165.8, 163.3, 159.9, 153.1, 151.9, 150.0, 145.0, 133.7, 132.0, 131.2, 126.7, 125.9, 123.3, 115.7, 114.8, 114.4, 114.5, 92.3, 88.4, 68.5, 56.3, 44.0, 30.2, 29.9, 29.1, 26.5, 25.7 ppm; FTIR (annealed film on CaF$_2$): $\tilde{\nu}$ = 3411, 3239, 3071, 3041, 2936, 2862, 2214, 1700, 1696, 1685, 1602, 1577, 1517, 1452, 1404, 1306, 1284, 1241, 1171, 1089, 1025 cm^{-1}; UV: λ_{max} = 291, 331, 353, 378 nm; photoluminescence (excitation at 340 nm, CHCl$_3$): 366, 384; DSC (T_m = 188 °C); MS (MALDI-TOF): m/z: 1012 [M^+].

4-(1-Hexyloxy-6-(N^6-(4-methoxybenzoyl)adenine)-1-bis(phenylethynyl)benzene (**A^{An}1bA^{An}**): The reaction was conducted according to the general procedure described above, using **A^{An}4b** (2.67 g, 4.36 mmol), and afforded a yellow solid. Column chromatography (silica gel; 1:99, 2:98→4:96 MeOH/CH$_2$Cl$_2$) of the resulting crude product afforded pure **A^{An}1bA^{An}** as a yellow solid (1.09 g, 50 %). ^{1}H NMR (CDCl$_3$, 200 MHz): δ = 9.10 (br s, 2H; NH), 8.78 (s, 2H; adenine H-8), 8.00 (d, 4H; anis-ArH), 7.98 (s, 2H; adenine H-2), 7.45 (d, 4H; ArH), 7.44 (s, 4H; ArH), 6.97 (d, 4H; anis-ArH), 6.85 (d, 4H; ArH), 4.26 (t, 4H; NCH$_2$), 3.95 (t, 4H; OCH$_2$), 3.87 (s, 6H; anis-OCH$_3$), 2.01–1.85 (m, 4H; NCH$_2$C*H*$_2$), 1.88–1.65 (m, 4H; OCH$_2$C*H*$_2$), 1.50–1.25 ppm (m, 20H; 10×alkyl CH$_2$); ^{13}C NMR (CDCl$_3$, 50 MHz): δ = 165.7, 164.8, 160.8, 154.0, 153.6, 151.2, 144.3, 134.7, 134.6, 132.8, 131.5, 127.4, 124.6, 124.5, 116.5, 116.1, 115.8, 115.7, 92.8, 89.5, 69.5, 57.0, 45.7, 31.5, 30.8, 30.7, 30.7, 30.5, 28.2, 27.5 ppm; FTIR (annealed film on CaF$_2$): $\tilde{\nu}$ = 3416, 3257, 3071, 3041, 2927, 2854, 2215, 1699, 1684, 1603, 1577, 1517, 1456, 1312, 1284, 1244, 1172, 1090, 1024 cm^{-1}; UV: λ_{max} = 290, 332, 352, 378 nm; photoluminescence (excitation at 340 nm, CHCl$_3$): 367, 385; DSC (T_m = 202 °C); MS (MALDI-TOF): m/z: 1098 [M^+].

4-(1-Hexyloxy-6-(N^3-methyl)-thymine)-1-iodobenzene (**T^{Me}4a**): Methyl iodide (174 μl, 0.28 mmol) was added in one portion to a stirred solution of DMF (3 mL), K$_2$CO$_3$ (0.19 g, 0.14 mmol), and **T4a** (0.30 g, 0.70 mmol) at 60 °C. After 16 h, the reaction was poured into water and extracted with CH$_2$Cl$_2$. The combined organic layers were washed with water and then the CH$_2$Cl$_2$ was evaporated. Column chromatography (silica gel; 99:1 CH$_2$Cl$_2$/MeOH) of the resulting crude product afforded pure **T^{Me}4a** (0.27 g, 88 %). M.p. 86 °C; ^{1}H NMR (CDCl$_3$, 300 MHz): δ = 7.55 (d, 2H; ArH), 6.96 (s, 1H; T-C*H*), 6.65 (d, 2H; ArH), 3.91 (t, 2H; OCH$_2$), 3.73

(t, 2H; NCH$_2$), 3.35 (s, 3H; T-NCH$_3$), 1.92 (s, 3H; T-CH$_3$), 1.84–1.65 (m, 4H; OCH$_2$C*H*$_2$ and NCH$_2$C*H*$_2$), 1.61–1.35 ppm (m, 4H; 2×alkyl CH$_2$); ^{13}C NMR (CDCl$_3$, 75 MHz): δ = 159.2, 138.4, 117.2, 82.7, 68.3, 34.3, 33.1, 29.6, 29.5, 29.4, 28.9, 28.4, 26.2. 164.2, 159.1, 151.8, 138.4, 117.1, 109.8, 103.6, 82.8, 68.0, 49.7, 29.3, 29.2, 28.2, 26.5, 25.9, 13.4 ppm; MS (MALDI-TOF): m/z: 443 [$M+H$]$^+$.

4-(1-Nonyloxy-6-(N^3-methyl)-thymine)-1-bis(phenylethynyl)benzene (**T^{Me}1aT^{Me}**): In a glove box, 1,4-diethynylbenzene (0.02 g, 0.15 mmol), **T^{Me}4** (0.08 g, 0.34 mmol), [Pd(PPh$_3$)$_4$] (2.00 mg, 1.71×10^{-6} mol), and CuI (1.00 mg, 1.71×10^{-6} mol) were added to a 3:1 v/v mixture of toluene/diisopropylamine (7.5 mL). The mixture was then heated to 75 °C, and stirred for 18 h under an argon atmosphere. The solvents of the resulting luminescent suspension were subsequently evaporated. Column chromatography (silica gel; 95:5 CH$_2$Cl$_2$/MeOH) of the resulting crude product afforded pure **T^{Me}1aT^{Me}** (0.12 g, 75 %). ^{1}H NMR (CDCl$_3$, 300 MHz): δ = 7.47 (s, 4H; ArH), 7.46 (d, 4H; ArH), 6.97 (s, 1H; T-C*H*), 6.86 (d, 4H; ArH), 3.98 (t, 4H; OCH$_2$), 3.71 (t, 4H; NCH$_2$), 3.37 (s, 6H; T-NCH$_3$), 1.95 (s, 6H; T-CH$_3$), 1.84–1.65 (m, 8H; OCH$_2$C*H*$_2$ and NCH$_2$C*H*$_2$), 1.60–1.35 ppm (m, 8H; 4×alkyl CH$_2$); ^{13}C NMR (CDCl$_3$, 75 MHz): δ = 164.3, 159.4, 151.8, 138.4, 133.4, 132.6, 131.7, 131.6, 124.9, 123.3, 121.25, 115.7, 114.8, 109.8, 91.5, 88.2, 68.0, 49.7, 29.3, 28.2, 26.5, 25.9, 113.4 ppm; FTIR (annealed film on CaF$_2$): $\tilde{\nu}$ = 3065, 2933, 2858, 2212, 1698, 1664, 1638, 1602, 1519, 1468, 1356, 1284, 1246, 1174 cm^{-1}; UV: λ_{max} = 274, 335, 354, 378 nm; photoluminescence (excitation at 330 nm, CHCl$_3$): 366, 383, 397; DSC (T_m = 154 °C); MS (MALDI-TOF): m/z: 754 [M^+].

N^7-Dodecyl-(N^6-(4-methoxybenzoyl)adenine (**dodecyl-A^{An}**): p-Anisoyladenine (2.33 g, 8.63 mmol) was dissolved in dry DMF (45.0 mL), and sodium hydride (1.00 g, 41.6 mmol) was added in portions. The mixture was allowed to stir for 1 h at RT. Bromododecane (3.98 mL, 16.0 mmol) was then added dropwise by means of a syringe and the mixture was allowed to stir for 5 h at 40 °C, followed by ~20 h at 30 °C. Methanol was added to deactivate any remaining NaH. The solvent was then evaporated, the residue was dissolved in CH$_2$Cl$_2$ and the organic phase was washed two times with water. Hexane was then added to the CH$_2$Cl$_2$ fraction and the product precipitated out upon removal of the CH$_2$Cl$_2$. The precipitate was filtered and reprecipitated again by using the same procedure. Column chromatography (silica gel; 99:1 CH$_2$Cl$_2$/MeOH) of the resulting crude product afforded pure dodecyl-A^{An} as a white solid (1.50 g, 40 %). M.p. 97 °C; R_f = 0.62 (95:5 CH$_2$Cl$_2$/CH$_3$OH); ^{1}H NMR (CDCl$_3$, 200 MHz): δ = 8.92 (br s, 1H; NH), 8.80 (s, 1H; adenine H-2), 8.15 (d, 2H; anis-ArH), 8.00 (s, 1H; adenine H-8), 7.02 (d, 2H; anis-ArH), 4.27 (t, 2H; alkyl ^{1}CH$_2$), 3.89 (s, 3H; anis-OMe), 2.05–1.82 (m, 2H; alkyl ^{2}CH$_2$), 1.42–1.12 (m, 8H; alkyl $^{(3–11)}$CH$_2$), 0.80–0.95 (t, 3H; alkyl CH$_3$); ^{13}C NMR (CDCl$_3$, 75 MHz): δ = 164.5, 163.4, 152.7, 152.3, 142.9, 130.2, 126.2, 123.2, 114.2, 55.7, 44.4, 32.2, 30.2, 29.8, 29.7, 29.6, 29.5, 29.3, 26.9, 22.9, 14.4 ppm; MS (MALDI-TOF): m/z: 439 [$M+H$]$^+$.

N^3-Dodecyl-thymine (**dodecyl-T**): Thymine (1.00 g, 7.93 mmol) was added to dry DMF (14 mL), and NaH (0.38 g, 15.8 mmol) was then added in portions to the mixture. The solution was thermostated at 100 °C for 4 h and then allowed to cool to RT. Bromododecane (4.37 mL, 18.2 mmol) was then added dropwise by means of a syringe, and the mixture was allowed to stir for 48 h at 100 °C. The reaction mixture was then removed from the heat and neutralized with ~2 mL of acetic acid. The solvent was evaporated in vacuo and the residue was dissolved in chloroform. Any remaining undissolved material was filtered off and the soluble fraction was then washed with water (100 mL). The separated chloroform was then stirred with sodium sulfate for 15 min and filtered. Hexane was then added to the CH$_2$Cl$_2$ fraction and the product precipitated out upon removal of the CH$_2$Cl$_2$. Column chromatography (silica gel; 99:1 CH$_2$Cl$_2$/MeOH) of the resulting crude product afforded pure dodecyl-**T** as a white solid (0.72 g, 30.7 %). M.p. 122.1 °C; R_f = 0.51 (95:5 CH$_2$Cl$_2$/CH$_3$OH); ^{1}H NMR (CDCl$_3$, 200 MHz): δ = 8.42 (br s, 1H; NH), 6.97 (s, 1H; T-CH), 3.70 (t, 2H; alkyl ^{1}CH$_2$), 1.95 (s, 3H; T-CH$_3$), 1.75–1.61 (m, 2H; alkyl ^{2}CH$_2$), 1.40–1.21 (m, 8H; alkyl $^{(3–11)}$CH$_2$), 1.95–1.85 ppm (m, 3H; alkyl ^{12}CH$_3$); ^{13}C NMR (CDCl$_3$, 50 MHz): δ = 166.2, 152.7, 142.0, 112,1, 50.1, 33.4, 31.1, 31.0, 30.9, 30.8, 30.7, 28.0, 24.3, 15.7, 14.0 ppm; MS (MALDI-TOF): m/z: 295 [$M+H$]$^+$.

Acknowledgements

[1] a) L. Brunsveld, B. J. B. Folmer, E. W. Meijer, R. P. Sijbesma, *Chem. Rev.* **2001**, *101*, 4071–4097; b) A. Ciferri, *Macromol. Rapid Commun.* **2002**, *23*, 511–529; c) *Supramolecular Polymers* (Ed.: A. Ciferri), Marcel Dekker, New York, **2000**.

[2] a) Z. Liang, O. M. Cabarcos, D. L. Allara, Q. Wang, *Adv. Mater.* **2004**, *16*, 823–827; b) H. Kosonen, J. Ruokolainen, M. Knaapila, M. Torkkeli, K. Jokela, R. Serimaa, G. ten Brinke, W. Bras, A. P. Monkman, O. Ikkala, *Macromolecules* **2000**, *33*, 8671–8675; c) A. Calzolari, R. Di Felice, E. Molinari, A. Garbesi, *Phys. E* **2002**, *13*, 1236–1239; d) G. N. Tew, M. U. Pralle, S. I. Stupp, *Angew. Chem.* **2000**, *112*, 527–531; *Angew. Chem. Int. Ed.* **2000**, *39*, 517–521; e) X. L. Chen, S. A. Jenekhe, *Macromolecules* **2000**, *33*, 4610–4612; f) J. B. Beck, S. J. Rowan, *J. Am. Chem. Soc.* **2003**, *125*, 13922–13923.

[3] a) T. Kato, *Supramol. Science*, **1996**, *3*, 53–59; b) T. Kato, J. M. J. Fréchet, *Macromol. Symp.* **1995**, *98*, 311–326; c) C. M. Lee, A. C. Griffin, *Macromol. Symp.* **1997**, *117*, 281–290; d) T. Kato, J. M. J. Fréchet, *J. Am. Chem. Soc.* **1989**, *111*, 8533–8534; e) T. Kato in *Handbook of Liquid Crystals* (Eds.: D. Demus, J. W. Goodby, G. W. Gray, H.-W. Spiess, V. Vill), Wiley-VCH, Weinheim, **1998**, Vol. *2B*, pp. 969–979; f) "Hydrogen-Bonded Liquid Crystals: Molecular Self-Assembly for Dynamically Functional Materials", T. Kato, *Struct. Bonding (Berlin)* **2000**, *96*, 95–146; g) Y. Kamikawa, M. Nishii, T. Kato, *Chem. Eur. J.* **2004**, *10*, 5942–5951.

[4] a) J.-M. Lehn, *Makromol. Chem. Macromol. Symp.* **1993**, *69*, 1–17; b) C. M. Paleos, D. Tsiourvas, *Angew. Chem.* **1995**, *107*, 1839–1855; *Angew. Chem. Int. Ed. Engl.* **1995**, *34*, 1696–1711; c) N. Zimmerman, J. S. Moore, S. C. Zimmerman, *Chem. Ind. (London)* **1998**, *15*, 604–610; d) M. Muthukumar, C. K. Ober, E. L. Thomas, *Science* **1997**, *277*, 1225–1232; e) *Struct. Bonding* (Ed.: M. Fujita), **2000**, *96*, whole volume; f) J.-M. Lehn, *Supramolecular Chemistry*, VCH, Weinheim, **1995**; g) A. Treybig, C. Dorscheid, W. Weissflog, H. Kresse, *Mol. Cryst. Liq. Cryst.* **1995**, *260*, 369–376; h) S. I. Torgova, A. Strigazzi, *Mol. Cryst. Liq. Cryst.* **1999**, *336*, 229–245; i) V. Percec, J. Heck, G. Johansson, D. Tomazos, M. Kawasumi, P. Chu, G. Ungar, *Mol. Cryst. Liq. Cryst. Sci.* **1994**, *254*, 137–196; j) V. Percec, *Macromol. Symp.* **1997**, *117*, 267–273; k) G. P. Spada, G. Gottarelli, *Synlett* **2004**, *4*, 596–602.

[5] a) L. Y. Park, D. G. Hamilton, E. A. McGehee, K. A. McMenimen, *J. Am. Chem. Soc.* **2003**, *125*, 10586–10590; b) K. A. McMenimen D. G. Hamilton, *J. Am. Chem. Soc.* **2001**, *123*, 6453–6454; c) R. K. Castellano, R. Clark, S. L. Craig, C. Nuckolls, J. Rebek, *Proc. Natl. Acad. Sci. USA* **2000**, *97*, 12418–12421; d) M. L. Bushey, T.-Q. Nguyen, W. Zhang, D. Horoszewski, C. Nuckolls, *Angew. Chem.* **2004**, *116*, 5562–5570; *Angew. Chem. Int. Ed.* **2004**, *43*, 5446–5453.

[6] J. M. Lehn, M. Mascal, A. DeCian, J. Fischer, *J. Chem. Soc. Chem. Commun.* **1990**, 479–481.

[7] C. Hilger, R. Stadler, *Polymer* **1991**, *32*, 3244–3249.

[8] C. He, A. M. Donald, A. C. Griffin, T. Waigh, A. H. Windle, *J. Polym. Sci. Part B: Polym. Phys.* **1998**, *36*, 1617–1624.

[9] M. J. Brienne, J. Gabard, J.-M. Lehn, I. Stibor, *J. Chem. Soc. Chem. Commun.* **1989**, 1868–1870.

[10] a) J.-M. Lehn, *Polym. Int.* **2002**, *51*, 825–839; b) T. Kato, N. Mizoshita, K. Kanie, *Macromol. Rapid Commun.* **2001**, *22*, 797–814; c) C. M. Paleos, D. Tsiourvas, *Liq. Cryst.* **2001**, *28*, 1127–1161; d) A. Ciferri, *Liq. Cryst.* **1999**, *26*, 489–494.

[11] a) T. Gulik-Krzywicki, C. Fouquey, J.-M. Lehn, *Proc. Natl. Acad. Sci. USA* **1993**, *90*, 163–167; b) P. Bladon, A. C. Griffin, *Macromolecules* **1993**, *26*, 6604–6610; c) M. Kotera, J.-M. Lehn, J.-P. Vigneron, *J. Chem. Soc. Chem. Commun.* **1994**, 197–199; d) M. Kotera, J.-M. Lehn, J.-P. Vigneron, *Tetrahedron* **1995**, *51*, 1953–1972; e) C. St. Pourcain, A. C. Griffin, *Macromolecules* **1995**, *28*, 4116–4121.

[12] S. Sivakova, S. J. Rowan, *Chem. Commun.* **2003**, 2428–2429.

[13] For examples of the use of DNA sequences in supramolecular polymerization processes, see: a) J. Xu, E. A. Fogleman, S. L. Craig, *Macromolecules* **2004**, *37*, 1863–1870; b) F. R. Kersey, G. Lee, P. Marszalek, S. L. Craig, *J. Am. Chem. Soc.* **2004**, *126*, 3038–3039; c) E. A. Fogleman, W. C. Yount, J. Xu, S. L. Craig, *Angew. Chem.* **2002**, *114*, 4198–4200; *Angew. Chem. Int. Ed.* **2002**, *41*, 4026–4028; d) S. M. Waybright, C. P. Singleton, K. Wachter, C. J. Murphy, U. H. F. Bunz, *J. Am. Chem. Soc.* **2001**, *123*, 1828–1833.

[14] For examples, see: a) W. Saenger, *Principles of Nucleic Acid Structures*, Springer, New York, **1984**; b) S. Sivakova, S. J. Rowan, *Chem. Soc. Rev.* **2005**, *34*, 9–21.

[15] K. Yamauchi, J. R. Lizotte, T. E. Long, *Macromolecules* **2002**, *35*, 8745–8750.

[16] S. J. Rowan, P. Suwanmala, S. Sivakova, *J. Polym. Sci. Part A: Polym. Chem.* **2003**, *41*, 3589–3596.

[17] W. H. Binder, M. J. Kunz, C. Kluger, G. Hayn, R. Saf, *Macromolecules* **2004**, *37*, 1749–1759.

[18] C. M. Paleos, J. Michas, *Liq. Cryst.* **1992**, *28*, 773–778.

[19] a) J. T. Davis, *Angew. Chem.* **2004**, *116*, 684–716; *Angew. Chem. Int. Ed.* **2004**, *43*, 668–698; b) T. Giorgi, F. Grepioni, I. Manet, P. Mariani, S. Masiero, E. Mezzina, L. Saturni, P. Sciaccini, G. P. Spada, G. Gottarelli, *Chem. Eur. J.* **2002**, *8*, 2143–2152, and references therein.

[20] For other studies of the interactions of N^6-substituted adenine derivatives, see: a) J. S. Nowick, T. Cao, G. Noronha, *J. Am. Chem. Soc.* **1994**, *116*, 3285–3289; b) J. S. Nowick, J. S. Chen, G. Noronha, *J. Am. Chem. Soc.* **1993**, *115*, 7636–7644; c) J. S. Nowick, J. S. Chen, *J. Am. Chem. Soc.* **1992**, *114*, 1107–1108.

[21] J. Sartorius, H.-J. Schneider, *Chem. Eur. J.* **1996**, *2*, 1446.

[22] R. K. Castellano, V. Gramlich, F. Diederich, *Chem. Eur. J.* **2002**, *8*, 118–129.

[23] A. R. A. Palmans, M. Eglin, A. Montali, C. Weder, P. Smith, *Chem. Mater.* **2000**, *12*, 472–480.

[24] G. W. Gray, J. W. G. Goodby, *Smectic Liquid Crystals: Textures and Structures*, Heyden & Son, Philadelphia, **1984**.

[25] J. Y Lee, P. C. Painter, M. M. Coleman, *Macromolecules* **1988**, *21*, 954–960.

[26] J. B. Lambert, H. F. Shurvell, D. A. Lightner, R. G. Cooks, *Organic Structural Spectroscopy*, Prentice Hall, New Jersey, **1998**.

[27] For a thermosensitive reversible polymer at the covalent level, see: a) X. Chen, M. A. Dam, K. Ono, A. Mal, H. Shen, S. R. Nut, K. Sheran, F. Wudl, *Science* **2002**, *295*, 1698–1702; b) X. Chen, F. Wudl, A. Mal, H. Shen, S. R. Nut, *Macromolecules* **2003**, *36*, 1802–1807.

[28] L. Kosynkina, T. Wei Wang, C. Liang, *Tetrahedron Lett.* **1994**, *35*, 5173–5176.